Fault Current Level Analysis of Future Microgrids with High Penetration Level of Power Electronic-Based Generation

Fault Current Level Analysis of Future Microgrids with High Penetration Level of Power Electronic-based Generation

Hussain Sarwar Khan
School of Technology and Innovations
University of vaasa
Vaasa, Finland
Hussain.khan@uwasa.fi

Khaled Syfullah Fuad
School of Technology and Innovations
University of vaasa
Vaasa, Finland
Khaled.Fuad@uwasa.fi

Mazaher Karimi
School of Technology and Innovations
University of vaasa
Vaasa, Finland
Mazaher.Karimi@uwasa.fi

Kimmo Kauhaniemi
School of Technology and Innovations
University of vaasa
Vaasa, Finland
Kimmo.Kauhaniemi@uwasa.fi

***Abstract*— The integration of power electronics-based generation has increased in the medium voltage (MV) level of the distribution networks, nowadays. It is obvious that the contribution level of this type of source is providing a limited fault current level according to the thermal and fault ride-through capability of power electronic converters. Therefore, the fault current level in the grid-connected and islanded mode of the microgrid is different and the protection scheme is required to be reviewed. In this regard, converters' responses contribute to the stability of the microgrid in the case of abnormal conditions. This paper has investigated the effect of power electronic converters and their controllers in future microgrids with the high penetration level of power electronic-based generation. A distribution management system has been designed to address the issues and challenges of faulty conditions and a voltage ride-through technique has been proposed. The simulation results of an MV distribution network demonstrate the fault current level of the future microgrid in abnormal conditions. The proper protection strategy is designed to detect any type of short circuit fault current as well as avoidance of damage to the integrated PEC-based generations.**

Keywords*— *Distribution management system, fault level detection, fault current, microgrid, power electronic converter-based generation, renewable energy sources, voltage ride-through

I. INTRODUCTION

Fault current is one of the important indicators in the traditional power system networks to detect any faulty conditions. The fault current level is high in the conventional power systems due to the fault level contribution of synchronous generators (SGs) [1, 2]. However, the integration of renewable energy sources (RESs) in recent years, due to the advantages of these types of generation, has been increased, exponentially. Electric power systems (EPSs) have experienced significant reformation, which has been particularly affected by an increased penetration level of power electronic converter (PEC) technologies. This reformation is in-line with the Paris agreement, as the European Council has defined the objective for the EU to be climate-neutral by 2050 [3]. As a matter of fact, EU members designed a plan to achieve this goal by reducing greenhouse gas emissions using RESs. PEC technologies are mostly used for RESs such as wind, photovoltaic generation, energy storage systems, etc. Implementation of RESs into the EPSs will results in high integration level of PEC-based generation into the EPS. In fact, the fast response of converters will affect the dynamic response and behavior of EPS. Despite the advantages of PEC-based generation, the fault current level will be reduced in EPS because of the low thermal capacity of PECs which limits the maximum output fault current to 1.1-2 time of the rated current whereas the SGs based sources inject 5-6 times of the rated current [4]-[5]. As a result, fault detection will be affected from the protection point of view and new strategies and adaptive protection are required in near future to overcome this issue.

Modern grid code and standards state that grid-connected RESs must be connected with the grid during faults in the grid side and have the capability of effective 'Fault ride-through (FRT)' to maintain stability at the power system level. The existing protection system based solely on fault current detection and PEC-based RESs with FRT capability affects the fault current level detection as shown in [2]. In fact, the FRT depends on the penetration level of the RESs, which are integrated in EPS. As a result, it will affect the existing protection system beyond the point of common coupling (PCC) as the fault level is higher at those points and can result in malfunctions in protection system.

A fault level calculation (FLC) method is proposed in [6] to find the effect of penetration of PECs based DERs to fault levels in transmission networks. The FLC method is based on the contribution of short circuit current from both SGs and PECs based RESs during a three-phase symmetrical fault. Fault contribution from SGs depends on the sub-transient reactance of SG and total line impedance between SG and the fault point. Two scenarios are considered as compound generation units at a certain bus where one SG and DERs are considered together as a unit and non-uniform penetration where DERs penetration is considered in all the bus along with SGs in the network. Calculated results show for the first scenario that during a three-phase symmetrical fault, the fault level at the closest bus decreases to 33% as the penetration level of DERs increases to 100%. Also, for the second scenario, the fault level at the closest bus decreases to 18% as the penetration level of DERs increases to 70%. The proposed method is also verified in an IEEE-39 bus system and compared with other conventional methods. Results show that the proposed FLC method calculated the fault level with less error compared to other methods like complete methods and IEC60909-based fault calculations. Also, it is

shown that buses close to the power generation unit experience a lower fault level than other remote buses. However, the exact location of the short circuit fault is not mentioned in the paper for calculation and simulation purposes. Also, only a three-phase short circuit is considered for the FLC method and tested for demonstration purposes.

The main goal of this paper is to demonstrate the effect of PEC-based generation on the fault level at MV distribution networks (DNs) operating as a microgrid both in grid-connected and islanded mode of operation. A distribution management system (DMS) has been developed to effectively manage the operation of microgrid in grid-connected or in islanding mode during normal operation and faulty conditions. Also, a voltage ride-through response controller (VRTRC) has been developed according to [7] and demonstrate the VRT capability of PEC-based generation. To the best of the authors' knowledge, no research has demonstrated the effect of PEC-based microgrid to the protection system in DNs. A DN model like Sundom Smart Grid [8] in Vaasa, Finland is modeled as precisely as possible with accessible data and grid structure in MATLAB/Simulink and PEC-based generations is integrated with the DN model to demonstrate the effect. At first, the control method of the PEC and the proposed DMS is described. Then, the test system and case studies are given. Finally, the simulation results for the proposed DMS has been demonstrated along with VRT application.

II. CONTROL METHOD OF THE PEC AND DISTRBUTION MANAGEMENT SYSTEM

The PEC-based RESs has been integrated into a MV distribution network, as a microgrid. Model predictive control (MPC) based voltage and current regulation loop is implemented for the control of the PEC-based RESs.

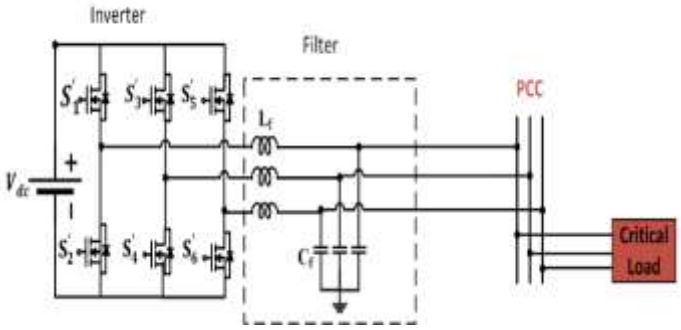

Fig. 1. Circuit diagram of voltage source converter.

a. Control model of the converter

Fig. 1 illustrates the circuit diagram of the voltage source converter that is consist of inverter and filter section and integrated into the EPS through PCC. MPC uses the mathematical model of system to find the optimal switching state for the PEC-based generation by minimizing the cost function. In this study, two-level voltage source inverter (VSI) is considered along with the LC filter. The two-level VSI has three legs with six switches and switching functions presented in (1-3).

$$S_x=\begin{cases}1, \text{ if } S_1' \text{ is ON and } S_2' \text{ is OFF}\\ 0, \text{ if } S_1' \text{ is OFF and } S_2' \text{ is ON}\end{cases} \quad (1)$$

$$S_y=\begin{cases}1, \text{ if } S_3' \text{ is ON and } S_4' \text{ is OFF}\\ 0, \text{ if } S_3' \text{ is OFF and } S_4' \text{ is ON}\end{cases} \quad (2)$$

$$S_z=\begin{cases}1, \text{ if } S_5' \text{ is ON and } S_6' \text{ is OFF}\\ 0, \text{ if } S_5' \text{ is OFF and } S_6' \text{ is ON}\end{cases} \quad (3)$$

Table 1 shows the possible voltage vectors aligned with switching states.

b. LC Filter

LC filter is used to suppress the switching harmonics. Here i_f represents the current through the inductor L and V_{pc} is the voltage across capacitor C_f. By applying the Kirchhoff's voltage and current law, change in current and voltage can be determined and stated in (4).

$$\frac{d}{dt}\begin{bmatrix} i_f \\ v_{PC}\end{bmatrix}=\mathbf{A}\begin{bmatrix} i_f \\ v_{PC}\end{bmatrix}+\mathbf{B}\begin{bmatrix} v_t \\ i_0\end{bmatrix} \quad (4)$$

TABLE 1. POSSIBLE VOLTAGE VECTORS ALIGNED WITH SWITCHING STATES

SPACE-VECTOR		ON-STATE SWITCHES	VECTOR PLACING
ZERO VECTOR	$\overrightarrow{V_{0,7}}$	S_1', S_3', S_5' S_4', S_6, S_2'	$\overline{v_{0,7}}=0$
ACTIVE VECTOR	$\overrightarrow{V_1}$	S_1', S_4', S_6'	$\overline{v_1}=\frac{2}{3}v_{dc}$
	$\overrightarrow{V_2}$	S_1', S_3', S_6'	$\overline{v_2}=\frac{1}{3}v_{dc}+j\frac{\sqrt{3}}{3}v_{dc}$
	$\overrightarrow{V_3}$	S_6', S_3', S_2'	$\overline{v_3}=-\frac{1}{3}v_{dc}+j\frac{\sqrt{3}}{3}v_{dc}$
	$\overrightarrow{V_4}$	S_2', S_3', S_5'	$\overline{v_4}=-\frac{2}{3}v_{dc}$
	$\overrightarrow{V_5}$	S_2', S_4', S_5'	$\overline{v_5}=-\frac{1}{3}v_{dc}-j\frac{\sqrt{3}}{3}v_{dc}$
	$\overrightarrow{V_6}$	S_1', S_5', S_4'	$\overline{v_6}=\frac{1}{3}v_{dc}-j\frac{\sqrt{3}}{3}v_{dc}$

Equation (4) represents the continuous state space model of filter and also expresses the dynamic effect of LC filter. In order to implement the model on digital platform Eq. (4) is converted into discrete time state space model with T_s as a sampling time. However, zero order hold approach is used [9].

$$\begin{bmatrix} i_f(t_k+1) \\ v_{PC}(t_k+1)\end{bmatrix}=\mathbf{A_d}\begin{bmatrix} i_f(t_k) \\ v_{PC}(t_k)\end{bmatrix}+\mathbf{B_d}\begin{bmatrix} v_t(t_k) \\ i_0(t_k)\end{bmatrix} \quad (5)$$

$$\mathbf{A_d}=e^{AT_s}, \mathbf{B_d}=\int_0^{T_s} e^{A\tau}\, B\, d_\tau \quad (6)$$

Equation (6) and (7) represent the discrete time model of the VSI with its LC filter. In the model, t_k represents the time instant and t_k+1 describes the future instant. The difference between both instants is equal to sampling time. T_S is considered as very small approaching to zero. So, exponential term is approximated as:

$$e^{AT_s} \approx 1 + AT_s \quad (7)$$

Capacitor voltage at following instant is calculated by using (6) and (8) and stated in (9).

$$v_{pc}(t_k+1) = v_{pc}(t_k) + \frac{T_s}{C_f}(i_f(t_k) - i_0(t_k)) \quad (8)$$

Cost function (CF) is the error between predicted voltage and the reference voltage. The algorithm calculates the CF for all seven voltage vectors as given in Table 1 [11]. The voltage vector, which has minimum value of CF among these, is selected and its switching sequence is given to VSI at coming instant. The CF is defined as:

$$g_v = (v^*_{pc,\alpha}(t_k) - v_{pc,\alpha}(t_k+1))^2 + (v^*_{pc,\beta}(t_k) - v_{pc,\beta}(t_k+1))^2 \quad (9)$$

$v_{pc,\alpha}$ and $v_{pc,\beta}$ are real and imaginary parts of predicted capacitor voltage. Inverter and filter parameterers are given in table 2. In the simulation, multiple inverter are conneted in parallel. So, parameter defined in table 2 is for single inverter.

TABLE 2. SIMULATION PARAMETERS

Parameters	Values
LC-filter	C_f=250μF,L_f=2mH
Damping Resistance	R_f=0.94Ω
Sampling Time	T_s=20μs
Rated Frequency	f_{nom}=50Hz
Nominal Voltage	V^6_{nom}= 575 V V^7_{nom} = 400 V
Inverter Rating	300 A

c. The proposed distribution management system

In this paper, a DMS is developed to detect any islanding condition for preparing the required actions to control the PEC-based RESs in the microgrid. The proposed flowchart of the DMS is illustrated in Fig. 2. In the DMS, the short circuit fault current will be detected based on the distance protection relays that has been proposed at the point of PEC-based connection (PoC). Then, the voltage ride-through response controller (VRTRC) of the DMS will check the performance and capability of the PEC-based RESs to fulfill the requirements for consecutive temporary voltage disturbances caused by short circuit faults in grid-connected and islanded conditions.

In Table 3, the maximum ride-through response time of the converters, which has been defined in [7], is presented. In the DMS, the VRTRC is designed to control the maximum ride-through response of the PEC-based generators for abnormal operating performance.

TABLE 3. VOLTAGE RIDE-THROUGH REQUIREMENTS FOR PEC-BASED GENERATION FOR ABNORMAL OPERATING PERFORMANCE

Voltage range (p.u.)	Maximum ride-through response time (s)
V>1.2	0.1
1.175<V≤1.2	0.2
1.1<V≤1.175	1
0.88≤V<1.1	Permissive Operation
0.7≤V<0.88	0.7
0.5≤V<0.7	0.16
V<0.5	0.1

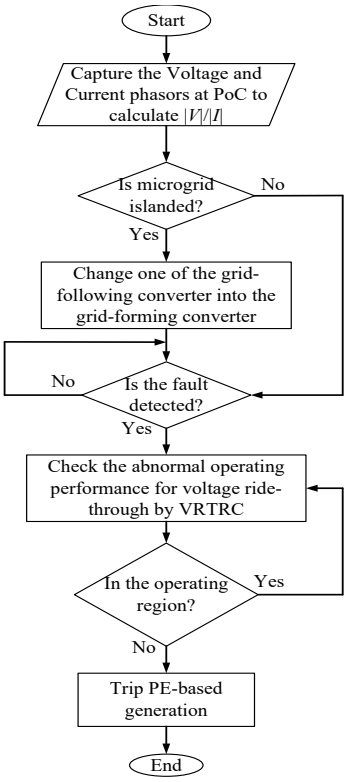

Fig. 2. The flowchart of the proposed DMS.

III. TEST SYSTEM AND CASE STUDIES

In order to study the effect of PEC-based RESs in abnormal conditions, a radial AC microgrid is chosen for simulation as a test system. Sundom Smart Grid is in Vaasa, Finland, and used as a smart pilot (http://ses.jrc.ec.europa.eu/sundom-smart-grid-ssg) that is modeled as a microgrid in this study [8]. This smart grid is consisting of an HV/MV substation and several feeders with regular loads, which are supplied also by a 2-MVA fully-rated converter-based wind turbine (Type-4, wind turbine) and 800-kVA photovoltaic (PV) solar panel. The single line diagram of the microgrid is presented in Fig. 3. The microgrid is connected with the transmission system through a transformer at bus 1. This bus is the point of connection between the main grid and the microgrid that is called the point of common coupling (PCC). A wind turbine generator is integrated with the microgrid at substation bus-6 through a converter with a 2-MVA capacity, whereas a photovoltaic generator is integrated at substation bus-7, which can supply the maximum power of 0.8 MVA. The points where the PEC-based RESs (bus-6 and bus-7) are electrically connected with the microgrid will be called PoC. The loads are also connected to buses 3, 4, and 5 with 20-kV distribution network feeders.

There are challenges in the microgrid protection and the fault level detection, especially for the microgrids that are capable to operate either in an islanded or grid-connected mode. In order to overcome these challenges, the islanding detection technique based on the measuring of the voltage and current at PoC is used

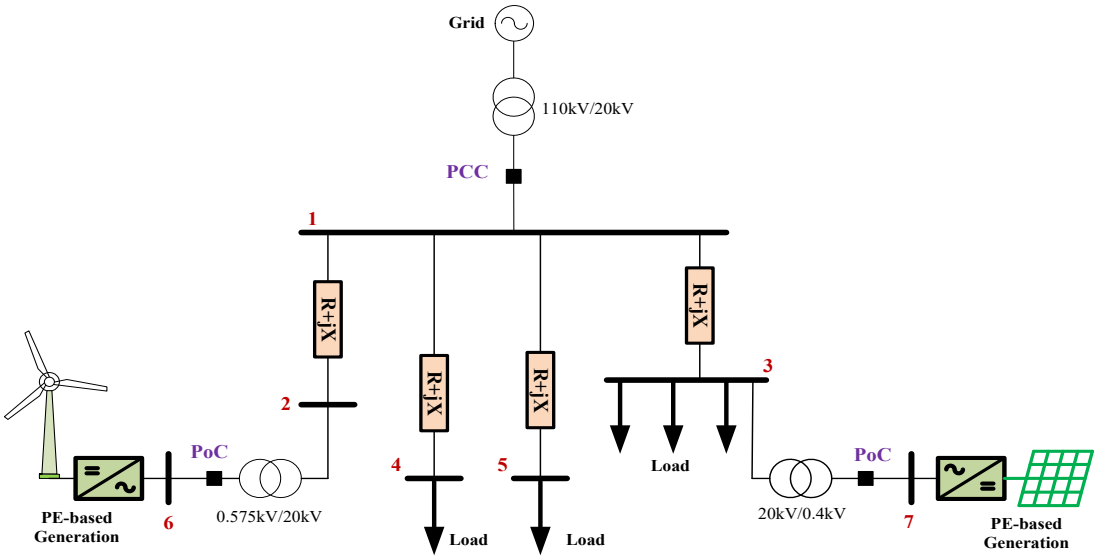

Fig. 3. A single line diagram model of the test system.

[10]. The method is decentralized, and it can be locally executed at each PEC-based RES terminal. The short circuit fault current level and voltage ride-through response are assessed in two different scenarios, *a)* grid-connected and *b)* islanded mode. In order to assess the short circuit fault current level, the three-phase fault is simulated in all substations for both scenarios.

IV. Results and Discussions

In this section, the PEC-based generation is integrated into the MV level of the microgrid (Sundom Smart Grid, see Fig. 3), and the simulation results are obtained. A 100% penetration level of the PEC-based generation is simulated in this paper to study the effect of PEC-based generation on the short circuit fault current. On the other hand, the voltage ride-through performance of the PEC-based generation is also assessed. The test system has been simulated in an islanded and grid-connected mode. The concept of this study is to apply faulty conditions in different buses in the test system. Then, the fault current level will be investigated, and a proper operating region of voltage ride-through will be assessed.

a. Grid-connected mode

In this mode, the microgrid is connected to the main grid at the PCC on bus number 1. Then, the proposed DMS is monitored PEC-based RESs of the test system at PoC, to detect any faulty condition using the distance protection relay. In this mode of operation, the voltage ride-through performance of the converters will be checked and the PEC-based generation will contribute to the fault current for a specified period according to the voltage range in Table 3. In the proposed DMS, it is possible to activate or disable the VRT response of the PEC-based generations in the grid-connected mode. In Fig. 4, the fault detection signal is presented that a faulty condition is detected at t=0.45 s with the duration of 200 ms.

In Fig. 5, the tripping signal of the VRTRC for the converter is presented and it has sent a disconnecting signal for converters at t=0.62 s. The DMS is detected the voltage sag at t=0.46 s as is depicted in Fig. 6. It can be seen that the proper signal is tripping the converters after 0.16 s according to Table 3. The tripping signal is generated by the VRTRC of the DMS in order to cease to energies the PEC-generations.

The short circuit fault current of the PEC-based generations and grid are presented in Fig. 7. In Figure 7 (a), the three-phase current of the PEC-based generation at bus 6 is presented and the VRTRC has not been activated to cease to energies for this generator. Unlike the PEC-based generation at bus 6, the VRTRC signal has been activated for the PEC-based generation at bus 7. Hence, as presented in Figure 7 (b), the proper signal, according to Table 3, trips the converter at t=0.6233 s. The fault current of the grid is also presented in Figure 7 (c). It can be seen that the fault current is mainly fed by the grid to the microgrid.

b. Islanding mode

To evaluate the proposed DMS, the microgrid is disconnected from the main grid at t=1 s. It is necessary to detect an islanding condition to change one of the converters from the grid-following mode into the grid-forming mode. The proposed DMS is responsible for detecting an islanding condition and sending the proper signals for the converter's controller. As it is mentioned earlier, at t=1 s the microgrid has been islanded and the DMS is detected the islanding operation mode of the microgrid at t=1.038 s, as is illustrated in Fig. 8.

It can be seen that it takes 0.038 s (less than 2 cycles) for the DMS to detect the islanding mode for changing one of the converters controllers into the grid-forming mode. Then, the three-phase fault is simulated at bus number 5. In Fig. 9, the fault detection signal is presented showing that a faulty condition is detected at t=1.5 s with the duration of 400 ms.

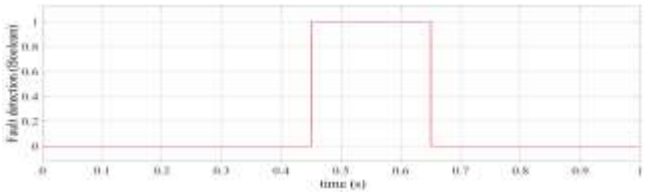

Fig. 4. The fault detection signal for case *a*

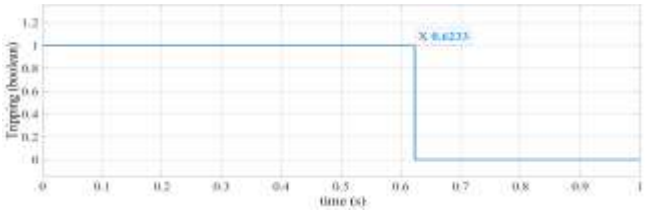

Fig. 5. The tripping signal of the VRTRC

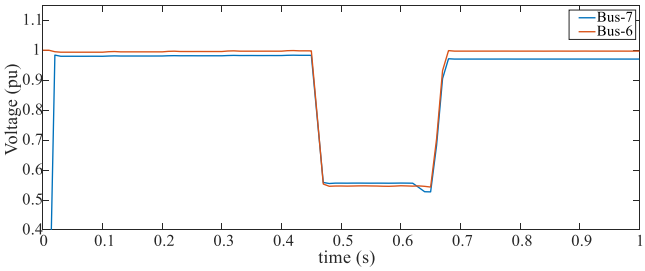

Fig. 6. The voltage sag at bus 6 & 7

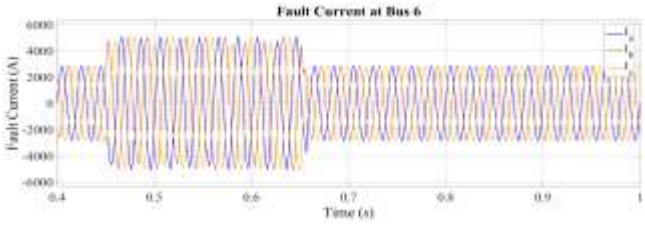

(a)

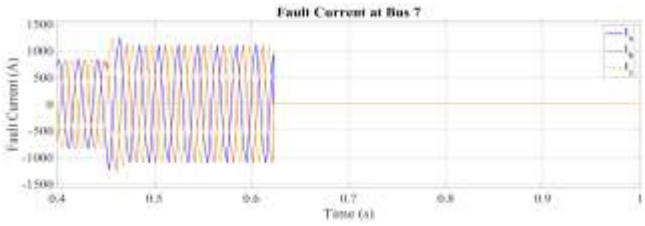

(b)

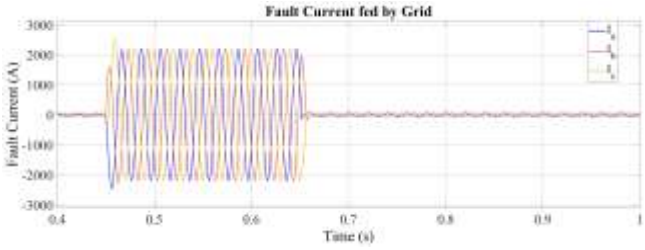

(c)

Fig. 7. The short circuit fault current: a) at bus 6, b) at bus 7, and c) current from the grid.

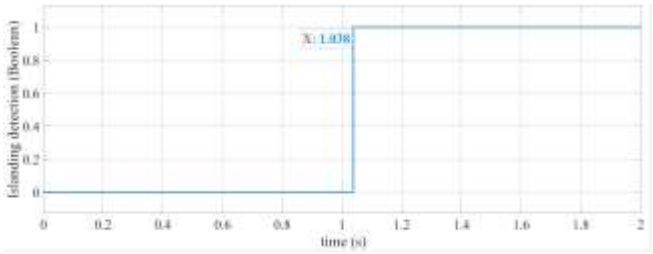

Fig. 8. The islanding detection signal

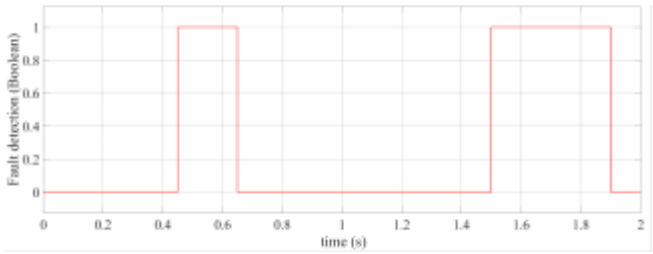

Fig. 9. The fault detection signal

The RMS value of the fault current is shown in Fig. 10. It can be seen that in the islanding mode of microgrid (t>1 s), the short circuit fault current level is reduced, dramatically. Due to the long duration of the faulty condition, in this case, the VRTRC of the DMS has detected the voltage sag at the PoC and used the maximum ride-through response time of the PEC-based generations during the fault condition.

The voltage magnitude in p.u. for the bus-6 and bus-7 is presented in Fig. 11. The tripping signal for the converter is shown in Fig. 12. The VRTRC has sent a disconnecting signal for converters at t=1.61 s. The VRTRC is detected the voltage sag at t=1.51 s as is depicted in Fig. 11. From this figure, it can be seen that the proper signal trips the converters after 0.1 s according to Table 3. The tripping signal is generated by the VRTRC of the DMS.

From the simulation results, it can be concluded that the proposed DMS was able to detect the faulty condition of the microgrid either in grid-connected or islanded mode; and the VRTRC is also successfully operating to utilize the capability of the PEC-based generations during the fault condition. The faulty condition of the islanded microgrid is repeated with the duration of 60 ms, in order to validate the capability of the VRTRC. The voltage of the bus-6 and bus-7 is illustrated in Fig. 13; and it proves that the fault ride-through current is requested from PEC-based generations by the VRTRC until the condition of Table 3 is fulfilled.

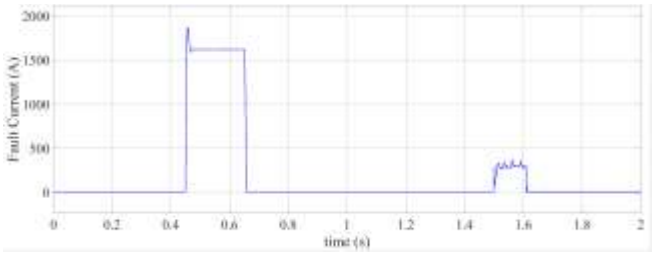

Fig. 10. The RMS value of the short circuit fault current

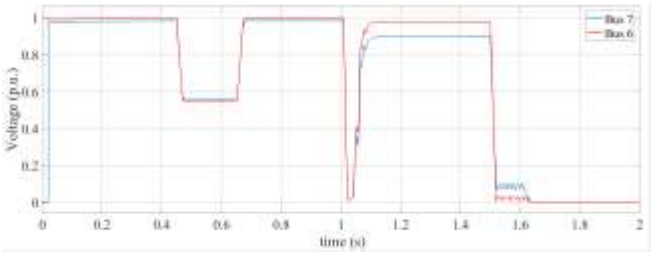

Fig. 11. The voltage magnitude for the buses 6 & 7

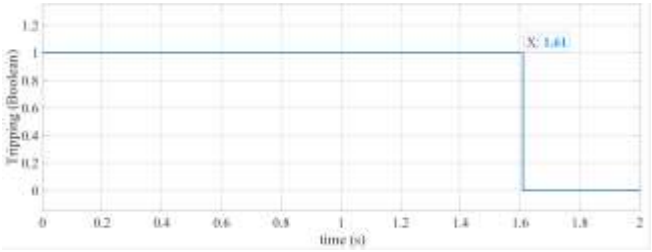

Fig. 12. Tripping signal of VRTRC for the converters

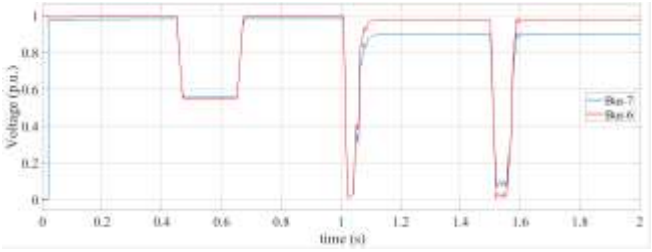

Fig. 13. The voltage magnitude for the buses 6 & 7

I. CONCLUSIONS

In this paper a DMS is proposed to demonstrate the operation of PEC-based RESs as microgrid in DNs in grid-connected and islanding mode during a three-phase fault. Results show that the proposed DMS effectively perform the VRT operation during the short circuit fault. It is also found that the PEC-based generation doesn't have significant contribution towards the fault current as expected. In this paper, we have considered the 100% penetration of PEC-based generations. Further investigation is needed to see the contribution of the PEC-based generation at different penetration levels of microgrid during balanced and unbalanced faults, which is left as future work

ACKNOWLEDGMENT

This work was carried out mainly in the Profi4/WP2 project with the financial support provided by the Academy of Finland. Some parts of this work were done in the SolarX research project with the financial support provided by the Business Finland with Grant No. 6844/31/2018. The financial support provided through these research projects is highly acknowledged.

REFERENCES

[1] R. Aljarrah, et al., "Issues and challenges of steady-state fault calculation methods in power systems with a high penetration of non-synchronous generation," Proceedings of the 2019 IEEE Milan PowerTech, Milan, Italy, pp. 1-6, 2019.

[2] T. Dragicevic, et al., "Advanced control methods for power converters in distributed generation systems and microgrids," IEEE Trans. Indust. Electron. 66(11), pp. 8866–8869, 2019.

[3] Pantelis, C., et al., "Energy-system modelling of the EU strategy towards climate-neutrality," Energy Policy, Vol. 134, 2019, https://doi.org/10.1016/j.enpol.2019.110960.

[4] V. Telukunta, J. Pradhan, A. Agrawal, M. Singh and S. G. Srivani, "Protection challenges under bulk penetration of renewable energy resources in power systems: A review," in CSEE Journal of Power and Energy Systems, vol. 3, no. 4, pp. 365-379, Dec. 2017.

[5] M. Usama et al., "A Comprehensive Review on Protection Strategies to Mitigate the Impact of Renewable Energy Sources on Interconnected Distribution Networks, " in IEEE Access, vol. 9, pp. 35740-35765, 2021.

[6] R. Aljarrah, et al., "Monitoring of fault level in future grid scenarios with high penetration of power electronics-based renewable generation," in IET Generation, Transmission & Distribution, vol. 15, pp. 177-382, January 2021.

[7] IEEE Standard for Interconnecting Distributed Resources with Electric Power Systems, IEEE Std. 1547-2018.

[8] H. Laaksonen, P. Hovila, "Future-proof islanding detection schemes in Sundom smart grid," 24th International Conference on Electricity Distribution, CIRED, Glasgow, 2017.

[9] H, Khan, et al. "Improved finite control set model predictive control for distributed energy resource in islanded microgrid with fault-tolerance capability." Engineering Science and Technology, an International Journal (2021).

[10] M. Karimi, et al., "An islanding detection technique for inverter-based distributed generation in microgrids," Energies, Vol. 14, 2021, https://doi.org/10.3390/en14010130.

[11] Khan, Hussain Sarwar, et al. "Finite control set model predictive control for parallel connected online ups system under unbalanced and nonlinear loads." Energies 12.4 (2019): 581.